A selectable, plasmid-based system to generate CRISPR/Cas9 gene edited and knock-in mosquito cell lines

Kathryn Rozen-Gagnon[1*], Soon Yi[1], Eliana Jacobson[1], Sasha Novack[1], and Charles M. Rice[1]

[1]Laboratory of Virology and Infectious Disease, The Rockefeller University, New York, NY 10065, USA

*Corresponding author: Kathryn Rozen-Gagnon. Phone (212) 327-7009. Fax (212) 327-7048. krozen@rockefeller.edu

Abstract

Aedes (Ae.) aegypti and *Ae. albopictus* mosquitoes transmit arthropod-borne diseases around the globe, causing ~700,000 deaths each year. Genetic mutants are valuable tools to interrogate both fundamental vector biology and mosquito host factors important for viral infection. However, very few genetic mutants have been described in mosquitoes in comparison to model organisms. The relative ease of applying CRISPR/Cas9 based gene editing has transformed genome engineering and has rapidly increased the number of available gene mutants in mosquitoes. Yet, *in vivo* studies may not be practical for screening large sets of mutants or possible for laboratories that lack insectaries. Thus, it would be useful to adapt CRISPR/Cas9 systems to common mosquito cell lines. In this study, we generated and characterized a mosquito optimized, plasmid based CRISPR/Cas9 system for use in U4.4 (*Ae. albopictus*) and Aag2 (*Ae. aegypti)* cell lines. We demonstrated highly efficient editing of the *AGO1* locus and isolated knock-down AGO1 cell lines. Further, we used homology-directed repair to establish knock-in Aag2 cell lines with a 3xFLAG-tag at the N-terminus of endogenous *AGO1.* These experimentally verified plasmids are versatile, cost-effective, and efficiently edit immune competent mosquito cell lines that are widely used in arbovirus studies.

Introduction

Mosquitoes from the genus *Aedes* are worldwide pests and major vectors of arthropod-borne viruses (arboviruses) that cause global human disease[1-3]. Notable members of this genus include *Ae. aegypti*, which transmits a wide variety of arboviruses, and *Ae. albopictus*, which is prevalent in North America and is an emerging vector for certain arboviruses, such as chikungunya virus[2,4,5]. The ability to perform functional genetic studies in mosquitoes and mosquito cells is crucial to our understanding of pro- and anti-viral mosquito host factors and for potential mosquito control

36 strategies[6-8]. Previous genome engineering in mosquitoes has been achieved using transposons[8-
37 11] and a variety of engineered nucleases such as transcription activator-like effector nucleases
38 (TALENs)[12,13], zinc-finger nucleases (ZFNs)[14-17]; and homing endonucleases (HEs)[6,18,19].
39 However, transposon-mediated transgenesis yields imprecise integrations and it can be laborious
40 to engineer nucleases for each target gene. Difficulties modifying mosquito genomes have been
41 compounded by their large and repetitive nature, which makes assembly and annotation a
42 struggle[20-23]. Therefore, despite their importance to human health, loss-of-function mutants in
43 mosquitoes have significantly lagged behind those available in model insects, such as *Drosophila*.
44
45 The adaptation of the bacterial type II clustered regularly interspaced short palindromic repeats
46 (CRISPR) and CRISPR-associated sequence 9 (Cas9) immune system for generalized gene
47 editing has revolutionized genome engineering[24-27]. In CRISPR/Cas9 gene editing, the
48 *Streptococcus pyogenes* Cas9 endonuclease is targeted to genomic DNA by complementary
49 guide RNAs, inducing double-stranded breaks (DSBs; for review of CRISPR/Cas9 see[24]).
50 Genomic loci with DSBs stimulate cellular DNA repair machinery that rejoins DSBs by non-
51 homologous end joining (NHEJ). NHEJ disrupts gene function through small insertions or
52 deletions. Alternatively, cellular homology-directed repair (HDR) can be used to correct the gene
53 or insert changes if a homologous donor template is present. The CRISPR/Cas9 system relies on
54 expression of Cas9, a CRISPR RNA (crRNA) that targets genomic DNA adjacent to a protospacer
55 adjacent motif (PAM; NGG motif) and a trans-activating CRISPR RNA (tracr RNA); crRNA and
56 tracrRNA are often provided together as a single guide RNA (sgRNA). Due to its relative ease of
57 adoption and high efficiency, CRISPR/Cas9-mediated gene editing has generated mutants and
58 knock-ins in a wide variety of cells and organisms[28-31], including *in vivo* in mosquitoes[32-36] (for
59 review see[37]). CRISPR/Cas9-mediated editing is a significant advance in the toolkit for functional
60 genetic studies in mosquitoes. However, not many laboratories have access to insectaries for *in*
61 *vivo* experiments, and initial validation of gene function in cells is more practical and cost effective

62 for examining large gene sets. Thus, it is desirable to establish mosquito adapted CRISPR/Cas9
63 plasmids to generate mutant or knock-in mosquito cell lines; such plasmids have not been
64 reported to-date.
65
66 Perhaps due to this lack of mosquito optimized plasmids, there have been relatively few (two)
67 reports of CRISPR/Cas9 edited mosquito cell lines. One study established a clonal cell line
68 (AF5)[38], which was then used to establish a Dicer-2 defunct AF5 subclone (AF139)[39]. The other
69 generated *Nix* gene loss-of-function and knock-in C6-36 cell lines[33]. However, these reports both
70 relied on *Drosophila* CRISPR/Cas9 plasmids[30] and contain no information on CRISPR/Cas9
71 editing efficiency. In the current study, we updated CRISPR/Cas9 plasmids that rely on *Drosophila*
72 promoters[29] with mosquito promoters for use in mosquito cells. We then applied this system in
73 widely utilized, immune-competent *Ae. aegypti* (Aag2)[40-42] and *Ae. albopictus* (U4.4)[42,43] cell lines.
74 Comparing mosquito adapted CRISPR/Cas9 plasmids to previously used *Drosophila* plasmids,
75 we demonstrated increased editing efficiency at the *AGO1* locus. We generated *AGO1*-edited,
76 knock-down U4.4 and Aag2 cell lines, as well as knock-in Aag2 cell lines that contain a 3xFLAG
77 tag at the N-terminus of endogenous *AGO1*. These well-characterized and efficient mosquito
78 optimized CRISPR/Cas9 plasmids will facilitate functional genetic studies in mosquito cell culture
79 systems.
80
81 **Results**
82
83 *Generation and characterization of mosquito optimized CRISPR/Cas9 plasmids*
84
85 To generate mosquito optimized plasmids for efficient CRISPR/Cas9 gene editing in mosquito
86 cells, we obtained a plasmid used in *Drosophila*, pDCC6[29]. This plasmid relies on two *Drosophila*
87 promoters to express CRISPR/Cas9 components: 1) the RNA Pol III *U6:96Ab*[29,44-48] (*dme* U6-2)

88 drives transcription of the sgRNA, and 2) the *hsp70Bb*[44,49] promoter (*dme* phsp70) drives
89 expression of the human codon-optimized *Streptococcus pyogenes* Cas9 (referred to as
90 hSpCas9[26,27,29,50]; Fig. 1a). Because robust hSpCas9 and sgRNA expression is essential for high-
91 efficiency editing, we replaced the *Drosophila* promoters in pDCC6 with appropriate *Ae. aegypti*
92 promoters.
93
94 We first replaced the *dme* phsp70 with the strong constitutive *Ae. aegypti* polyubiquitin promoter
95 (*aae PUb*[15,32,51]; Fig. 1b). Expression of hSpCas9 in this intermediate plasmid (pKRG2) was then
96 assessed in comparison to the parental pDCC6 plasmid (Fig. 1c,d). We observed increased
97 expression of hSpCas9 in both Aag2 and U4.4 cells using the mosquito PUb promoter. The *dme*
98 phsp70 promoter has long been applied to mosquito cells and, notably, the first stable
99 transformations of mosquito cell lines was performed using this promoter[52]. However, the reported
100 frequency of transformants was quite low, an observation possibly explained by the lower levels
101 of expression we observed from *dme* phsp70 in mosquito cells.
102
103 We next updated the U6 promoter to drive sgRNA expression (Fig. 1e). The *Drosophila* U6-2
104 promoter in the pDCC6 plasmid[29], which was also used to generate prior CRISPR/Cas9-edited
105 mosquito cells[33,39], is quite ineffective in mosquito cell lines[53]. We selected the previously
106 described *Ae. aegypti*-derived U6 promoter, *AAEL017774*[54], which is effective in mosquito cells[53].
107 These two promoter replacements generate the backbone of the mosquito optimized pKRG3
108 plasmid (pKRG3-mU6-PUb-3xFLAG-hSpCas9). Because the N-terminal 3xFLAG tag on the
109 hSpCas9 may be undesirable for some applications, we also generated a pKRG3 plasmid with
110 this tag removed (pKRG3-mU6-PUb-hSpCas9).
111
112 Finally, we added a selectable marker to pKRG3. Although we optimized transfections
113 (representative transfection of U4.4 shown in Supplementary Fig. 1), no estimates of

114 CRISPR/Cas9-mediated editing efficiency have been reported in mosquito cells. Thus, it may be
115 essential to select transfected cells to increase the likelihood of editing. We generated a plasmid
116 expressing hSpCas9 fused to a selectable marker, a puromycin resistance cassette (pAc). The
117 pAc was inserted after the well-characterized insect virus *Thosea asigna* T2A[55] '2A-like' ribosome
118 skipping site. This T2A has been applied in *Drosophila* S2 and mosquito (C6/36 and Aag2)
119 cells[30,33,39,56,57], and was the most efficient skipping site in a comparison of five 2A variations in
120 *Drosophila*[58]. This design ensures co-expression of the hSpCas9 and the pAc selectable marker
121 under one strong, constitutive mosquito promoter (pKRG3-mU6-PUb-hSpCas9-pAc).
122
123 To assess the suitability of puromycin selection in Aag2 and U4.4 cells, we performed puromycin
124 kill curves to titrate the optimal concentration (data not shown). Puromycin treatment killed both
125 cell lines efficiently in the absence of pAc expression, and PUb-driven expression of hSpCas9-
126 pAc significantly increased cell viability in the presence of puromycin (Fig. 2a,b). We additionally
127 confirmed efficient T2A skipping in both mosquito cell lines by examining the size of hSpCas9 by
128 immunoblot (Fig. 2c,d). In both cases, the hSpCas9 was processed correctly and we observed a
129 strong band at the expected size (~160 kDa) in both constructs. The slight shift in hSpCas9-pAc
130 is due to additional amino acids in the T2A upstream of the skipped residue, and is consistent
131 with T2A processing in Drosophila[56]. A higher nonspecific band is present in all lanes and does
132 not reflect unprocessed hSpCas9-pAc, which would run at ~185 kDa. Therefore, PUb-Cas9-pAc
133 constructs correctly express and process hSpCas9 and enable rapid selection in U4.4 and Aag2
134 cells.
135
136 *Efficient CRISPR/Cas9 editing of* AGO1 *in U4.4 cells using mosquito-adapted plasmids*
137
138 As proof-of-principle, we investigated whether the mosquito optimized pKRG3 CRISPR/Cas9
139 plasmid would enable editing of U4.4 cells at the *AGO1* locus. Guides were designed against the

140 experimentally determined U4.4 genomic sequence near the *AGO1* translational start site by
141 searching for PAM NGG sequences. Because no U4.4 genome has been published, we first
142 verified the starting methionine to target by 5'RACE (this differed from the annotated start site;
143 unpublished results). Three guides were designed in the first exon near the beginning of the
144 coding sequence in order to disrupt *AGO1* (Fig. 3a). Guides were cloned into pKRG3 and these
145 plasmids were transfected singly or in combination into U4.4 cells (Fig. 3b). Post-puromycin
146 selection, we assessed editing efficiency by surveyor assay (Fig. 3c). In this assay, mismatches
147 between annealed wild-type (WT) and edited amplicons leads to cleavage by the surveyor
148 nuclease. Un-transfected WT cells exhibited the expected amplicon at ~350 bp (black arrow; and
149 a smaller, nonspecific band). In contrast, U4.4. cells transfected with pKRG3 plasmids revealed
150 a slightly lower band (red arrow) in addition to the WT band. This indicates amplification of both
151 WT and CRISPR/Cas9 edited *AGO1* loci from pKRG3-transfected cells. We observed that editing
152 was not equally efficient for all single guides, although they were all designed in close proximity.
153 Further, combinatorial transfections with two or three guides performed by far the best[44,47,48]. For
154 a head-to-head comparison, we additionally examined editing using the same hSpCas9
155 expression and puromycin selection conditions with the *dme* U6-2 promoter (pKRG2) instead of
156 the *aae* U6 promoter (pKRG3). When guides were expressed from the *dme* U6-2 promoter we
157 did not observe any editing, even using all three guides in combination. Therefore, in U4.4 cells
158 the pKRG3 plasmid substantially increases editing efficiency compared to plasmids that rely on
159 *dme* U6-2 for sgRNA expression.
160
161 We next isolated single U4.4 cell clones from this edited population to establish clonal cell lines
162 and assess their potential edits and AGO1 protein level (Fig. 3d). Sequencing of clonal lines
163 showed disruptive edits corresponding to sgRNA cleavage sites (~65% of clones were edited;
164 example alignment shown in Supplementary Fig. 2a). Immunoblot showed decreased protein
165 levels in several of the isolated clones compared to WT levels (Fig. 3d, top). Consistently, we

166 observed that most clones with lower AGO1 levels were isolated from cell populations transfected
167 with combinations of guides. Detection of an ectopically expressed 3xFLAG-tagged U4.4 AGO1
168 confirmed detection of mosquito AGO1 using the immunoblot antibody (Fig. 3d, bottom).
169 Interestingly, we were unable to isolate a complete knock-out clone despite isolating a variety of
170 different edited lines.
171
172 To confirm that reduced AGO1 protein levels corresponded with reduced AGO1 function, we
173 performed a microRNA (miRNA) reporter assay. In mosquitoes, small, host encoded miRNAs
174 direct AGO1 to repress imperfectly complementary transcripts[59]. We assessed whether U4.4 WT
175 or knock-down AGO1 clones could use endogenous miR-34 to repress a *Renilla* luciferase
176 reporter gene containing miR-34 target sequences (Fig. 3e). Several of the knock-down clones,
177 but neither WT clone, exhibited consistently reduced repression. These data indicate that
178 mosquito optimized CRISPR/Cas9 plasmids can be used to edit *AGO1* and to reduce AGO1
179 protein function in U4.4 cells.
180
181 *CRISPR/Cas9 mediates efficient editing and allows knock-in of* AGO1 *in Aag2 cells*
182
183 We next asked whether mosquito adapted plasmids would also allow editing of *Ae. aegypti* Aag2
184 cells. Additionally, we aimed to generate a knock-in *AGO1* Aag2 cell line by applying
185 CRISPR/Cas9 editing and providing a homology-directed repair (HDR) donor template. To do so,
186 as in U4.4, we designed three guide RNAs near the *AGO1* starting methionine (Fig. 4a).
187 Additionally, we designed an HDR donor template to insert an N-terminal 3xFLAG tag at the
188 endogenous *AGO1* locus (Fig. 4b). Because HDR can be very inefficient, upstream of the 3xFLAG
189 we inserted a red fluorescent protein (RFP) driven by the PUb promoter, flanked by two loxP sites.
190 This allows sorting of RFP positive cells to isolate potentially rare clones with the PUb-RFP-
191 3xFLAG integrated. The PUb-RFP marker can then be excised via expression of Cre

192 recombinase, leaving only a small scar upstream of the 3xFLAG-tagged *AGO1*. This entire
193 cassette was flanked by ~1kb of homology on either terminus[30].
194
195 Aag2 cells were transfected with pKRG3 plasmids singly or in combination, with the linearized
196 HDR donor template (Fig. 4b). As in U4.4 cells, editing efficiency of bulk Aag2 cells was assessed
197 post-puromycin selection. In contrast to in U4.4 cells, in Aag2 cells we consistently observed high
198 editing efficiency whether guides were expressed singly or in combination (Fig. 4c). Isolation of
199 single cell clones followed by sequencing showed ~28% of isolated clones contained edits
200 (example alignment shown in Supplementary Fig. 2b). Immunoblot showed several clones with
201 decreased and one clone with ablated AGO1 expression (Fig. 4d, top). We were able to detect
202 3xFLAG-tagged short and long Aag2 AGO1 isoforms by ectopic expression or constitutive
203 expression in stably transformed cell lines, confirming reliable detection of mosquito AGO1 (Fig.
204 4d, bottom). Unfortunately, the single AGO1 knock-out clone grew poorly and could not be
205 expanded to sufficient cell numbers to establish a knock-out cell line. We were, however, able to
206 establish AGO1 knock-down Aag2 clonal cell lines, as with U4.4.
207
208 After transfection and selection, cells were cultured for ~one week, until the input HDR donor
209 template RFP signal diminished. Cells were then sorted to identify clones that were RFP positive
210 due to knock-in of the donor template (Fig. 4b). The efficiency of HDR was very low and only
211 ~0.1% of cells were RFP positives. We screened RFP positive single cell clones by PCR and
212 identified two homozygous clones (B2 and C10) with the correct integration, indicated by a ~3700
213 bp product (compared to the WT amplicon of ~1500 bp; Fig. 4e). Our primer design outside of the
214 homology arms ensured that this screening PCR only detects the integrated HDR donor template.
215 To excise the loxP-PUb-RFP-loxP cassette, we transfected cells with a plasmid expressing a
216 puromycin-selectable Cre recombinase using the PUb promoter (pKRG4-mPUb-Cre-pAc; Fig. 4f).
217 Upon Cre expression, ~50% of the selectable cassette was excised; this percentage could be

218 increased by selecting for Cre transfected cells with puromycin. To generate the final 3xFLAG-
219 tagged *AGO1* knock-in cell lines, RFP-negatives, which were abundant, were again sorted
220 following Cre transfection and selection (Fig. 4g). PCR of established B2 and C10 subclones
221 indicated homozygous excision. Therefore, CRISPR/Cas9 editing and HDR were applied to
222 commonly used Aag2 cells to knock-in a 3xFLAG tag at the N-terminus of the endogenous *AGO1*
223 locus.
224
225 **Discussion**
226
227 This study provides the first detailed overview and optimization of CRISPR/Cas9 editing in
228 mosquito cells. We generated a set of versatile, selectable CRISPR/Cas9 plasmids, updated for
229 use in mosquito cells. First, by replacing the *Drosophila* hsp70 promoter with the *Ae. aegypti*
230 promoters, we demonstrated increased Cas9 expression in both mosquito cell lines examined.
231 We also verified correct processing of the T2A ribosomal skipping site, enabling constitutive Cas9
232 and pAc expression from the same PUb promoter (Fig. 2). This strategy was previously employed
233 to generate CRISPR edited Aag2 cells and C6/36 cells, using the same Cas9-T2A-pAc under the
234 *Drosophila* Actin-5c promoter[30,33,39]. We showed that expression of hSpCas9 or Cre fused to T2A-
235 pAc conferred resistance to puromycin and that puromycin treatment increased the desired cell
236 population (Fig. 2, 4). Second, we replaced the *dme* U6-2 promoter with an *aae* promoter for
237 sgRNA expression. Although we saw high levels of editing of the *AGO1* locus using the *aae* U6
238 promoter, we could not detect any editing using the *dme* U6-2 promoter used in the prior mosquito
239 cell studies[33,39]. This observation is consistent with previous results that the *dme* U6-2 promoter
240 is not very active in mosquito cells[53]. Thus, the mosquito optimized CRISPR plasmids reported
241 here are a significant improvement upon the *Drosophila*-based plasmids previously used in
242 mosquito cells[33,39].
243

244 Interestingly, in contrast to observations in mosquitoes *in vivo*[32], our results suggest that a single-
245 plasmid CRISPR system works well in mosquito cells. Using the updated mosquito CRISPR/Cas9
246 plasmids, we obtained ~28-65% edited *AGO1* clones. Co-delivery and expression of both
247 hSpCas9 and sgRNAs from the same, selectable plasmid may increase editing efficiency.
248 Ultimately, high editing efficiencies reduce the labor involved expanding and screening clones,
249 enabling functional interrogation of larger gene sets. Further, selecting bulk edited cells rather
250 than starting with a clonal cell line for editing[39] allows isolation of multiple WT and knock-out or -
251 down clonal cell lines. Surveying multiple WT and edited clones gives an accurate impression of
252 the phenotypic variation obtained for a given gene mutant from cell to cell. For example, we
253 observed reduced ability to repress miR-34 reporters for the majority of AGO1 knock-down U4.4
254 clones, but observed variability in the degree of AGO1 impairment. Despite high editing efficiency
255 of the *AGO1* locus in both cell types examined, we were only able to isolate knock-down clones.
256 This is consistent with the impaired growth observed for some miRNA-deficient mammalian cells[60]
257 and suggests selective pressure against complete *AGO1* knock-outs. Notably, we were also able
258 to use CRISPR/Cas9 plasmids in combination with an HDR donor template to generate Aag2
259 *AGO1* knock-in cells. Although the efficiency of HDR-mediated integration was low, 0.1% was still
260 sufficiently high to isolate *AGO1* knock-in Aag2 cells. Further, the robust CRISPR/Cas9 system
261 we report will permit future optimization of HDR efficiency in mosquito cells. The ability to knock-
262 in large cassettes and excise them allows further flexibility in tagging endogenous proteins for
263 mechanistic studies or generating conditional knock-outs in mosquito cells.
264
265 In all, we generated a versatile, effective, single plasmid system for the generation of
266 CRISPR/Cas9 edited mosquito cell lines. The mosquito adapted plasmids we report are a cost-
267 effective tool to screen and investigate functional phenotypes for a large number of gene mutants.
268 This easily customizable set of plasmids can also be updated to encode different Cas9 variants
269 for other applications, such as blocking gene transcription (CRISPR interference) or increasing

270 gene expression (CRISPR activation). It is our hope that this system will facilitate functional
271 genetic studies using widely accessible, immune-competent cell models for major vectors of
272 arboviruses.
273
274 **Methods**
275
276 *Cell lines*
277
278 Mosquito U4.4 (*Ae. albopictus*) and Aag2[40] (*Ae. aegypti*) cell lines were kind gifts from Dr. Dennis
279 Brown and from Dr. Maria Carla Saleh, respectively. Cell lines were grown in Leibovitz's L-15
280 Medium, no phenol red (Thermo Fisher Scientific), supplemented with 20% (U4.4) or 10% (Aag2)
281 fetal bovine serum (FBS, Hyclone, GE Healthcare), 0.1 mM non-essential amino acids (Thermo
282 Fisher Scientific), and ~0.3g/L tryptose phosphate broth (Sigma-Aldrich) at 28°C, 0% CO_2.
283
284 *Plasmid generation*
285
286 All CRISPR/Cas9 plasmids were generated from the pDDC6 plasmid, which encodes the human
287 codon-optimized *Streptococcus pyogenes* Cas9 (*hSpCas9*[29,50]; a gift from Peter Duchek
288 (Addgene plasmid #59985; http://n2t.net/addgene:59985; RRID:Addgene_59985). All oligos and
289 gBlocks Gene Fragments were purchased from IDT (see Supplementary Table 1 for all oligo and
290 gBlock sequences). All restriction enzymes, calf intestinal phosphatase (CIP), T4 DNA ligase and
291 Gibson Assembly Master Mix were purchased from NEB, and digests and ligations were
292 performed according to the manufacturer's protocol. Polymerase chain reactions (PCRs) were
293 performed using Phusion DNA polymerase (NEB) according to manufacturer's protocols. All
294 transformations were performed using in-house DH5alpha chemically competent cells according
295 to standard protocols. Plasmids were isolated from bacteria using the QIAprep Spin Miniprep Kit

296 (Qiagen) and DNA purifications were performed using QIAquick Gel Extraction and QIAquick PCR
297 Purification Kits (Qiagen), all according to the manufacturer's protocols. All plasmids were
298 sequence-verified and pKRG3 sequences and the HDR donor template sequence are available
299 in the Supplemental Information.
300
301 To replace the *dme* phsp70 promoter (*hsp70Bb*[44,49]) in pDCC6 with the *Ae. aegypti* polyubiquitin
302 promoter (*aae PUb*[15,32,51]), an *AfeI* site was introduced by site-directed mutagenesis using the
303 QuikChange II XL kit (Agilent) and oligos RU-O-22971 and RU-O-22972. The region containing
304 the *Afe1* site was then cloned into a clean pDCC6 background by digestion of the parental pDCC6
305 and pDCC6-AfeI with flanking sites *SapI/AvrII* followed by ligation, transformation, and DNA
306 isolation. *Aae* Pub with flanking *AfeI/AvrII* sites was amplified using RU-O-22977 and RU-O-
307 22978 and Phusion polymerase (NEB) from the plasmid pSL1180-HR-PUbECFP[15,32] (a gift from
308 Leslie Vosshall; Addgene plasmid # 47917; http://n2t.net/addgene:47917;
309 RRID:Addgene_47917). The resulting plasmid, pKRG2 (pKRG2-dU6-PUb-3xFLAG-hSpCas9),
310 was sequence verified and contains the *dme* U6-2 promoter (*Drosophila* Pol III promoter
311 *U6:96Ab*[44,45]) and the *aae* PUb promoter driving expression of hSpCas9.
312
313 To replace the *dme* U6-2 promoter with the *Aae. aegypti* U6 promoter (*aae* U6; *AAEL017774*[54]),
314 we had to alter the sgRNA cloning sites due to an internal *BbsI* site in the *aae* U6. We designed
315 primers to add an overhang corresponding to the *aae* U6 to a modified sgRNA cloning site that
316 relies on *BsmBI* to the pKRG2 sgRNA tracrRNA (trans-activating CRISPR RNA) scaffold and
317 terminator sequence, with a downstream *Afe*I site (RU-O-22974 and RU-O-22975). The scaffold
318 PCR and a gBlocks Gene Fragment containing the *aae* U6 sequence and an upstream *SacI* site
319 were assembled by Gibson assembly. The assembled DNA was PCR amplified using primers
320 RU-O-22975 and RU-O-22976. The *aae* U6 insert and pKRG2 were digested with *SacI/AfeI*,
321 ligated, and DNA was isolated to obtain pKRG3-mU6-PUb-3xFLAG-hSpCas9, which contains the

322 *aae* U6 promoter driving sgRNA expression and the *aae* PUb promoter driving expression of
323 hSpCas9.
324
325 We additionally generated a version of this plasmid with the 3xFLAG at the beginning of the Cas9
326 removed. To remove the 3xFLAG, we introduced a *NcoI* site by site-directed mutagenesis using
327 oligos RU-O-23100 and RU-O-23101. We then cloned this mutagenized insert into a clean
328 pKRG3 background by restriction enzyme digest with *BglII*/*XhoI*. The pKRG3-NcoI plasmid was
329 then digested with *NcoI* to remove the 3xFLAG and re-ligated to generate pKRG3-mU6-PUb-
330 hSpCas9. We made another variation with the puromycin resistance cassette (pAc) added. We
331 amplified the end of Cas9, the intervening T2A sequence[56], and pAc from pAc-sgRNA-Cas9[30] (a
332 gift from Ji-Long Liu; Addgene plasmid #49330; http://n2t.net/addgene:49330;
333 RRID:Addgene_49330) using primers RU-O-23782 and RU-O-23783. We then digested pKRG3
334 with *Eag1/BsrGI* and generated pKRG3-mU6-PUb-hSpCas9-pAc by Gibson assembly. For
335 comparative purposes, we also removed the 3xFLAG and added the pAc to hSpCas9 in pKRG3
336 by the same method, generating pKRG2-dU6-PUb-hSpCas9-pAc.
337
338 To generate overexpression plasmids as positive controls for mosquito AGO1 immunoblotting,
339 the pKRG3 plasmid was further modified. Aag2 N-terminal 3xFLAG-tagged short and long AGO1
340 isoforms and the U4.4 N-terminal 3xFLAG-tagged AGO1 with pKRG3 plasmid overhangs were
341 PCR-amplified from an in-house plasmid containing experimentally validated AGO1 sequences
342 in each cell line (unpublished data). The hSpCas9 sequence was removed from pKRG3-mU6-
343 PUb-hSpCas9-pAc by digestion with *NcoI*/*BsrGI* and AGO1 sequences were inserted by Gibson
344 assembly. Alternatively, to generate an empty pKRG3 plasmid, the ends of the *NcoI/BsrGI*-
345 digested plasmid were filled with T4 DNA polymerase (NEB) according to the manufacturer's
346 protocol and blunt ends were re-ligated. Finally, the *aae* U6 sequence was removed from pKRG3
347 Ago-containing or empty plasmids by digestion with *SapI/AfeII*; the ends were filled with T4 DNA

348 polymerase and blunt ends were ligated. This generated an empty, all-purpose pKRG4-mPUb-
349 pAc plasmid, as well as pKRG4-mPUb-3xFLAG-Aag2-AGO1-short-pAc, pKRG4-mPUb-3xFLAG-
350 Aag2-AGO1-long-pAc, and pKRG4-mPUb-3xFLAG-U44-AGO1-pAc. To express Cre
351 recombinase for excision of the fluorescent reporter between the loxP sites, Cre recombinase
352 was amplified from pME66 (a gift from S. Sarbanes) using primers adding *SacI/AvrII* sites; the
353 Cre insert and pKRG4-mPUb-pAc were digested with *SacI*/*AvrII* to generate pKRG4-mPUb-Cre-
354 pAc.
355
356 *CRISPR guide RNA design and cloning*
357
358 To design CRISPR RNAs (crRNAs) corresponding to *AGO1* (*Ae. aegypti* AaegL3 genome
359 assembly, AaegL3.3 annotations, *AAEL012410*; *Ae. albopictus* AaloF1 assembly, AaloF1.2
360 annotations, *AALF020776),* we confirmed the genomic sequence around the experimentally
361 determined translational start site in each cell line (unpublished data from 5'RACE and cDNA
362 sequencing). Aag2 and U4.4 cell genomic DNA was isolated using the DNeasy Blood & Tissue
363 Kit (Qiagen) according to the manufacturer's protocol. Aag2 genomic DNA was amplified using
364 primers RU-O-22776 and RU-O-22777, designed using the *Ae. aegypti* AaegL3 assembly, which
365 has the correct annotated starting methionine. U4.4 genomic DNA was amplified using primers
366 RU-O-22929 and RU-O-22931, designed using the *Ae. albopictus* AaloF1 assembly, where we
367 could only identify a downstream methionine in 5'RACE experiments. Three guide oligos
368 containing the *BsmBI* overhangs in pKRG3 plasmids were designed for each cell line based on
369 protospacer adjacent motif (PAM) NGG sequences in close proximity to the starting methionine
370 (RU-O-23427 to RU-O-23434, *Ae. aegypti*; RU-O-23456 to RU-O-23463, *Ae. albopictus*). The
371 parent pKRG3-mU6-PUb-hSpCas9-pAc plasmid was digested with *BsmBI* and annealed oligos
372 were ligated to generate 6 pKRG3 plasmids, one for each guide, according to protocols from
373 Kistler et al., 2015 and Cornell's Stem Cell and Transgenic Core Facility

374 (https://transgenics.vertebrategenomics.cornell.edu/genome-editing.html). These co-express the
375 crRNA plus the tracrRNA as a single guide RNA (sgRNA), and hSpCas9.
376
377 *Cloning of homology-directed repair (HDR) donor template*
378
379 The pSL1180-HR-PUbECFP plasmid was used as the backbone for cloning an HDR donor
380 template. A 2kb homology arm fragment around the translational start site of AGO1 in Aag2 cells
381 was amplified from Aag2 genomic DNA using oligos RU-O-24703 and RU-O-24704, to add
382 homology with the pSL1180-HR-PUbECFP plasmid. We ordered a gBlocks Gene Fragment
383 containing an inserted 3xFLAG-tag between the first methionine and the second amino acid of
384 AGO1, with silent mutations to ablate the sgRNA PAM sites. The gBlock extended past
385 *PpuMI/EagI* sites in the homology arm. Next, the homology arm was digested with *PpuMI/EagI* to
386 drop out the central ~160 nt, generating 2 ~1kb homology fragments overlapping the gBlock.
387 pSL1180-HR-PUbECFP was digested with *NotI/EcoRI*, dropping out the PUB-eCFP, and the
388 fragments were assembled to generate the intermediate plasmid pSL1180-HR-Aag2-3xFLAG-
389 AGO1. Next, pSL1180-HR-Aag2-3xFLAG-AGO1 was modified to add the loxp-PUb-RFP-loxP
390 cassette, with overlaps corresponding to the upstream homology arm and downstream 3xFLAG-
391 AGO1 sequence. We generated four PCRs: PCR1) 5'HA-loxP primers = RU-O-25019 and RU-
392 O-25020, template = pSL1180-HR-Aag2-3xFLAG-AGO1 pSL1180-HR-Aag2-3xFLAG-AGO1);
393 PCR2: loxP-PUB-RFP (primers= RU-O-25021 and RU-O-25022, template = pKRG3), PUb-RFP-
394 loxP (primers = RU-O-25023 and RU-O-25024, template= pTRIPZ; Dharmacon), loxP-3xFLAG-
395 3'HA (primers = RU-O-25027 and RU-O-25028, template = pSL1180-HR-Aag2-3xFLAG-AGO1).
396 pSL1180-HR-Aag2-3xFLAG-AGO1 was digested with *KpnI/PpuMI* and the fragments were
397 assembled by Gibson assembly to generate pSL1180-HR-Aag2-loxP-PUb-RFP-loxP-3xFLAG-
398 AGO1.
399

400 *General transfections*

401

402 Aag2 and U4.4 cells were transfected with the appropriate plasmids using Fugene HD
403 Transfection Reagent (Promega) according to the manufacturer's protocol. Cells were seeded at
404 ~50% confluency and complexes were formed using a ratio of 3:1 transfection reagent to plasmid
405 DNA. In the case of transfection with multiple clones, the total DNA concentration was kept
406 constant and individual plasmids were mixed at equal concentrations.

407

408 *Cell survival assays*

409

410 Cells were seeded at 50% confluency into 96-well plates and transfected with no plasmid, an
411 eCFP control plasmid lacking the pAc (pSL1180-HR-PUbECFP), or a PUb-hSpCas9-pAc plasmid
412 (pKRG2). Day 2 post-transfection, media was replaced with puromycin-containing media (2.5
413 ug/mL for Aag2 cells and 10ug/mL for U4.4 cells). At Day 0,1,2, and 3 post-puromycin addition,
414 cell survival was analyzed using the CellTiter-Glo Luminescent Cell Viability Assay (Promega)
415 and a FLUOstar Omega Microplate Reader (BMG LABTECH), according to the manufacturer's
416 instructions. Luciferase values at each day post-puromycin addition were normalized by plasmid
417 paired untreated controls. Survival at each day by plasmid was further normalized to the
418 measured survival for that plasmid at Day 0. Five replicates were collected per condition. Data
419 were analyzed using two-way analysis of variance (ANOVA) with Dunnett's *post hoc* test,
420 compared to the transfection control without plasmid (Prism 8).

421

422 *Generation of stable cell lines*

423

424 To generate Aag2 cells stably expressing the long AGO1 isoform with an N-terminal 3xFLAG tag,
425 Aag2 cells were transfected with pKRG4-mPUb-3xFLAG-Aag2-AGO1-long-pAc. Day 2 post-

426 transfection, Aag2 cells were treated with a low concentration of puromycin (1 ug/mL) and
427 maintained until cultures recovered (~2 weeks). 3xFLAG-tagged AGO1 expression was confirmed
428 by immunoblot in polyclonal transformants.
429
430 *CRISPR/Cas9 transfections*
431
432 Mosquito cells were transfected with pKRG3-mU6-PUb-hSpCas9-pAc plasmids each containing
433 an AGO1 sgRNA singly, or in combination. Day 2 post transfection, puromycin-containing media
434 was added (2.5 ug/mL, Aag2; 10 ug/mL, U4.4) and cells were selected for an additional 2 days.
435 Post-selection, cell pellets were collected and screened for editing efficiency.
436
437 For Aag2 knock-in cells, transfections were performed as above but linearized pSL1180-HR-
438 Aag2-loxP-PUb-RFP-loxP-3xFLAG-AGO1 (*XcmI/AflII)* was co-transfected.
439
440 *Surveyor assays*
441
442 Genomic DNA was isolated from bulk cells transfected with CRISPR/Cas9 plasmids using the
443 epicentre QuickExtract DNA Extraction Solution (Lucigen) according to the manufacturer's
444 protocol. PCRs were amplified from genomic DNA using primers RU-O-22929 and RU-O-24042
445 were used for U4.4 cells (full-length PCR product = 353 bp, digested = ~330 bp + ~23 bp); primers
446 RU-O-22776 and RU-O-22777 were used for Aag2 cells (full-length PCR product = 412 bp,
447 digested = ~179 bp + ~231 bp). PCRs were screened for editing efficiency using the Surveyor
448 Mutation Detection Kit (IDT) according to the manufacturer's instructions, and treated amplicons
449 were visualized on ~1% agarose gels with 100 bp DNA ladder (NEB) and SYBR Gold (Thermo
450 Fisher Scientific).
451

452 *Single cell cloning*

453

454 For bulk CRISPR/Cas9-transfected cells with apparent editing, we isolated single cells to
455 establish clonal edited cell lines. This was done by serial dilution: in brief, cells were resuspended
456 to a concentration of ~7 cells/mL and aliquoted into 96-well plates (~0.7 cells/well) in 50% fresh
457 media, and 50% conditioned media. Cells were expanded and screened by PCR (primers RU-O-
458 22929 and RU-O-24042) and Sanger sequencing (Macrogen).

459

460 To isolate knock-in 3xFLAG tagged *AGO1* Aag2 cell lines, cells were resuspended at 2E6/mL in
461 FACS cell sorting buffer (complete L-15 supplemented with 10mM HEPES, 5 mM EDTA and
462 40ng/mL DAPI). Live, RFP positive cells were sorted for integration of the donor template. Live,
463 RFP negative cells were sorted post Cre transfection and excision. All sorting was performed
464 using a BD FACSAria II sorter (BD Biosciences) with a 100um nozzle and a sheath pressure of
465 ~20 lbf/in^2 into 96-well plates containing 50% fresh media, and 50% conditioned media. Cells were
466 expanded and genomic DNA was isolated and screened for integration or excision by PCR
467 (primers RU-O-26075 and RU-O-26076); amplicons were visualized on ~1% agarose gels with 1
468 kb plus DNA ladder (NEB) and SYBR Gold (Thermo Fisher Scientific). WT DNA generates a band
469 of ~1460 bp, DNA with HDR-mediated integration of the donor template generates a band of ~700
470 bp, and Cre excised DNA generates a band of ~1500 bp). The same PCR was used to Sanger-
471 sequence (Genewiz) B2 and C10 knock-in cell lines to confirm the correct sequence post-
472 integration and post-excision.

473

474 *Editing efficiency estimates*

475

476 The percent of edited clones reported was calculated by sequencing isolated clones (primers RU-
477 O-22776 and RU-O-22777, Aag2; primers RU-O-22930 and RU-O-22931, U4.4). The number of

478 clones that had mixed traces or deletions at sgRNA cleavage sites was calculated over the total
479 number of clones sequenced (Aag2 = 26/93, U4.4 = 8/13).
480
481 *SDS-PAGE and immunoblot*
482
483 Potentially edited clone cell pellets were collected alongside positive control cell pellets. For Aag2
484 cells, positive controls were Aag2 cells transfected with pKRG4-3xFLAG-Aag2-short or the stable
485 Aag2-3xFLAG-AGO1-long cell line. For U44, cells were transfected with pKRG4-3xFLAG-U44.
486 Pellets were lysed in ice-cold 1X PXL lysis buffer (0.1% SDS, 0.5% sodium deoxycholate, 0.5%
487 NP-40 in 1X PBS) plus protease inhibitor (cOmplete, Mini Protease Inhibitor Cocktail Tablets,
488 EDTA free, Roche) on ice for 10 minutes and clarified by centrifugation at 15,000 rpm for 20
489 minutes at 4°C. Supernatants were collected and total protein was determined by BCA assay
490 (Pierce BCA Protein Assay Kit, Thermo Scientific) using a FLUOstar Omega Microplate Reader
491 (BMG LABTECH). 10 ug protein/sample was diluted in 1X LDS Sample Buffer and 50 mM DTT
492 (Sigma-Aldrich), then incubated for 10 minutes at 70°C. Samples were loaded on 4-12% Bis-Tris
493 gels and run in 1X MOPS SDS Running Buffer in the Mini Gel Tank according to manufacturer's
494 Precision Plus Protein Dual Color Standards (Bio-Rad). Following electrophoresis, protein was
495 transferred (Blot Module Set, Thermo Fisher Scientific) onto 0.2 μM nitrocellulose (Amersham
496 Protran Premium, GE Healthcare) according to manufacturer's protocol. Blots were developed
497 using fluorescent detection (LI-COR) with the following primary antibodies: anti-*Drosophila* AGO1
498 ab5070 (Abcam), anti-*Ae. aegypti* AGO1 (generated in-house), anti-Cas9 ab204448 (Abcam),
499 and anti-FLAG (monoclonal M2, Sigma-Aldrich). Following development membranes were
500 imaged (Odyssey CLX, LI-COR).
501
502 *Luciferase reporter assays*

503

504 To assay miRNA-mediated silencing in U4.4 knock-down CRISPR clones, reporters were cloned
505 corresponding to 4x miR-34-5p ideal target sites (8mer target followed by 4 mismatches, RU-O-
506 24800 and RU-O-24801) or one perfect miR-34-5p target site (RU-O-24794 and RU-O-24795).
507 Oligos were annealed and inserted into the *NotI/XhoI*-digested psiCHECK2 plasmid (Promega).
508 1E5 cells/well were plated in 48-well plates and transfected with empty, perfect, or 4x ideal
509 reporters. Day 2 post-transfection, cells were harvested and analyzed using the Dual-Luciferase
510 Reporter Assay System (Promega) and a FLUOstar Omega Microplate Reader (BMG LABTECH),
511 according to the manufacturer's instructions. The *Renilla* luciferase (RLuc) signal in each well was
512 normalized to that well's firefly luciferase (FLuc) signal to measure repression. Then the
513 RLuc/Fluc ratio was normalized to the ratio obtained with the empty reporter in each cell line
514 (which is the unrepressed ratio for that U4.4 clone). To compare normalized ratios to U4.4 clones
515 with WT AGO1 expression, we then divided each clone's normalized ratio per reporter by the
516 average ratio for that reporter obtained with our two WT clones to obtain a measurement of
517 silencing efficiency. Transfections were performed in triplicate and data were analyzed using two-
518 way analysis of variance (ANOVA) with Dunnett's *post hoc* test, compared to the WT clone sg1
519 A (Prism 8).

520

521 **Data Availability**

522

523 The cell lines generated and datasets analyzed during the current study are available from the
524 corresponding author on reasonable request. Plasmid sequences are provided in the
525 Supplementary Information file and pKRG3 and *AGO1* HDR donor plasmids are being deposited
526 to addgene; until the deposit is complete, plasmids are available upon request.

Figure 1. Mosquito optimized CRISPR/Cas9 plasmids.

(a) pDCC6 plasmid published in Gokcezade et al., 2014. The *dme* U6-2 promoter drives sgRNA transcription and the *dme* phsp70 promoter drives expression of a 3xFLAG-tagged hSpCas9. Guide RNAs are cloned by *BbsI* digest.

(b) pKRG2 plasmid, generated by replacing the *dme* phsp70 promoter with the *aae* PUb promoter. Cloning of guide RNAs as in (a).

(c) Immunoblot of Aag2 cells treated with transfection reagent (ctrl) or transfected with pDCC6 (3xFLAG-hSpCas9; expressed from the *dme* pshp70 promoter) or with pKRG2 (3xFLAG-hSpCas9; expressed from the PUb promoter). kDa = kilodaltons. Full-length blots in Supplementary Fig. 3.

(d) As in (c) for U4.4 cells.

(e) To generate pKRG3 mosquito adapted plasmids, the pKRG2 guide RNA cloning site was redesigned to use *BsmBI* (allowing insertion of the *aae* U6 promoter, which is incompatible with the *BbsI* sgRNA cloning site). The RNA Pol II *aae* U6 promoter was then inserted to express sgRNAs. This plasmid was further modified by removing the N-terminal 3xFLAG from Cas9 and adding a T2A-pAc to allow puromycin selection to yield several options for mosquito optimized CRISPR/Cas9 editing.

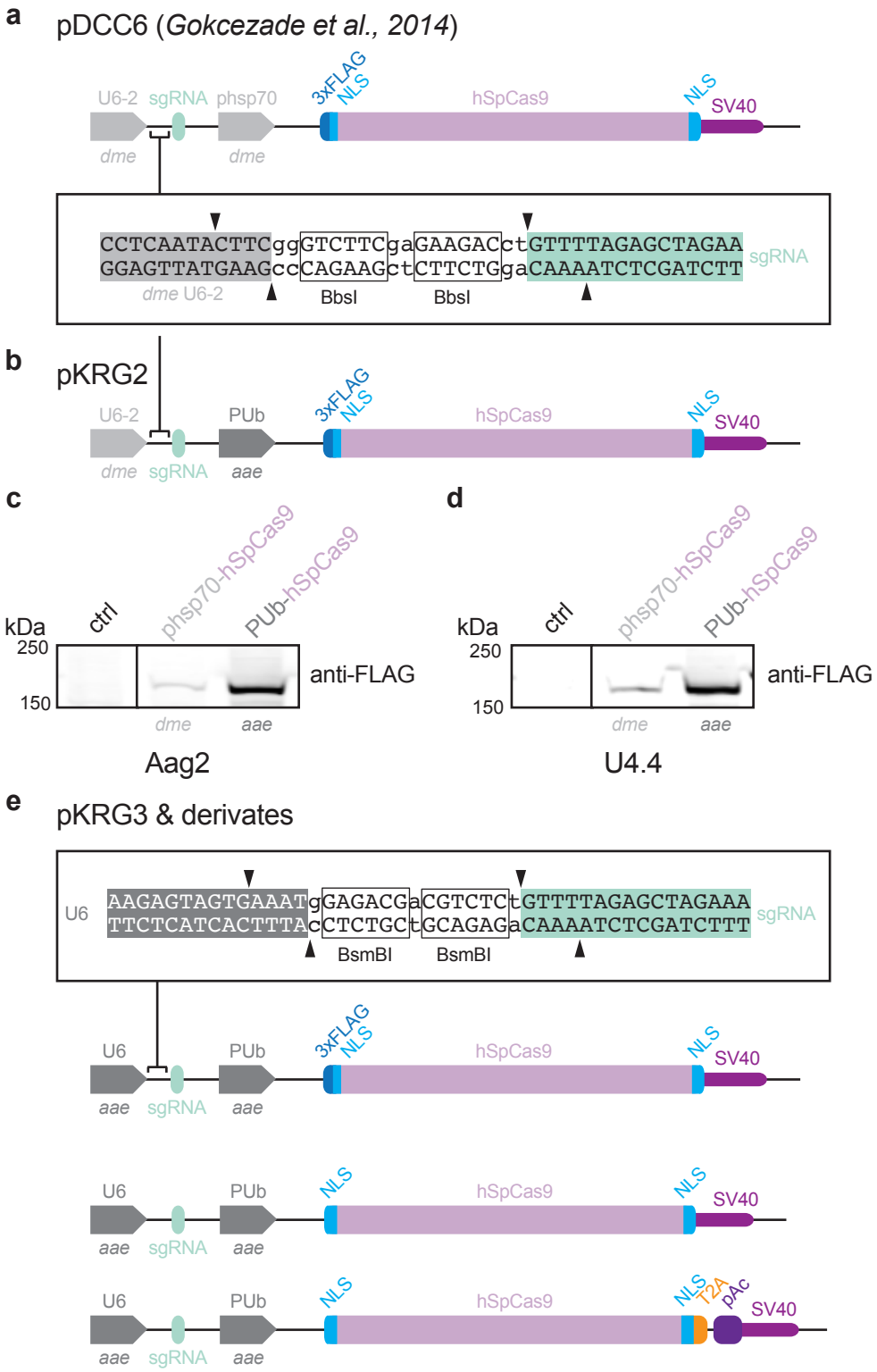

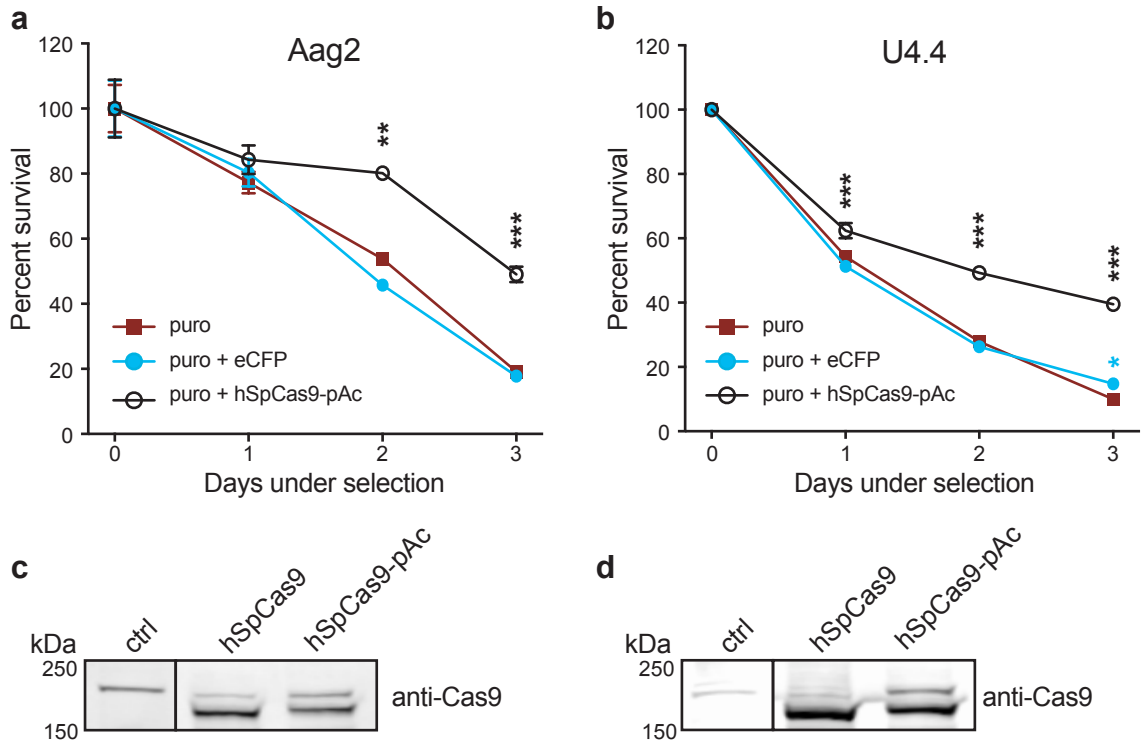

Figure 2. Efficient puromycin selection of hSpCas9-pAc transfected mosquito cells.

(a) Aag2 cells were pre-treated with transfection reagent alone (puro), transfected with a control PUb-eCFP (enhanced cyan fluorescent protein) plasmid lacking a puromycin resistance cassette (puro + eCFP), or transfected with PUb-hSpCas9 linked to a puromycin resistance cassette by the T2A skipping site (hSpCas9-pAc). Day 2 post-transfection, cells were treated with 2.5 ug/mL puro (puromycin). $P < 0.0001$ (overall ANOVA comparing different transfections); individual groups were compared using the Dunnett's *post hoc* test compared to the puro control; $^{**}P < 0.001$, $^{***}P \leq 0.0001$.

(b) As in (a) for U4.4 cells treated with 10 ug/mL puro. $^{*}P < 0.05$, $^{***}P \leq 0.0001$.

(c) Immunoblot of Aag2 cells treated with transfection reagent alone (ctrl) or transfected with hSpCas9 or hSpCas9-pAc (driven by PUb promoter). Expected size of hSpCas9 is ~160 kilodaltons (kDa); expected size of unprocessed hSpCas9-pAc is ~185 kDa. Full-length blots in Supplementary Fig. 3.

(d) As in (c) for U4.4 cells.

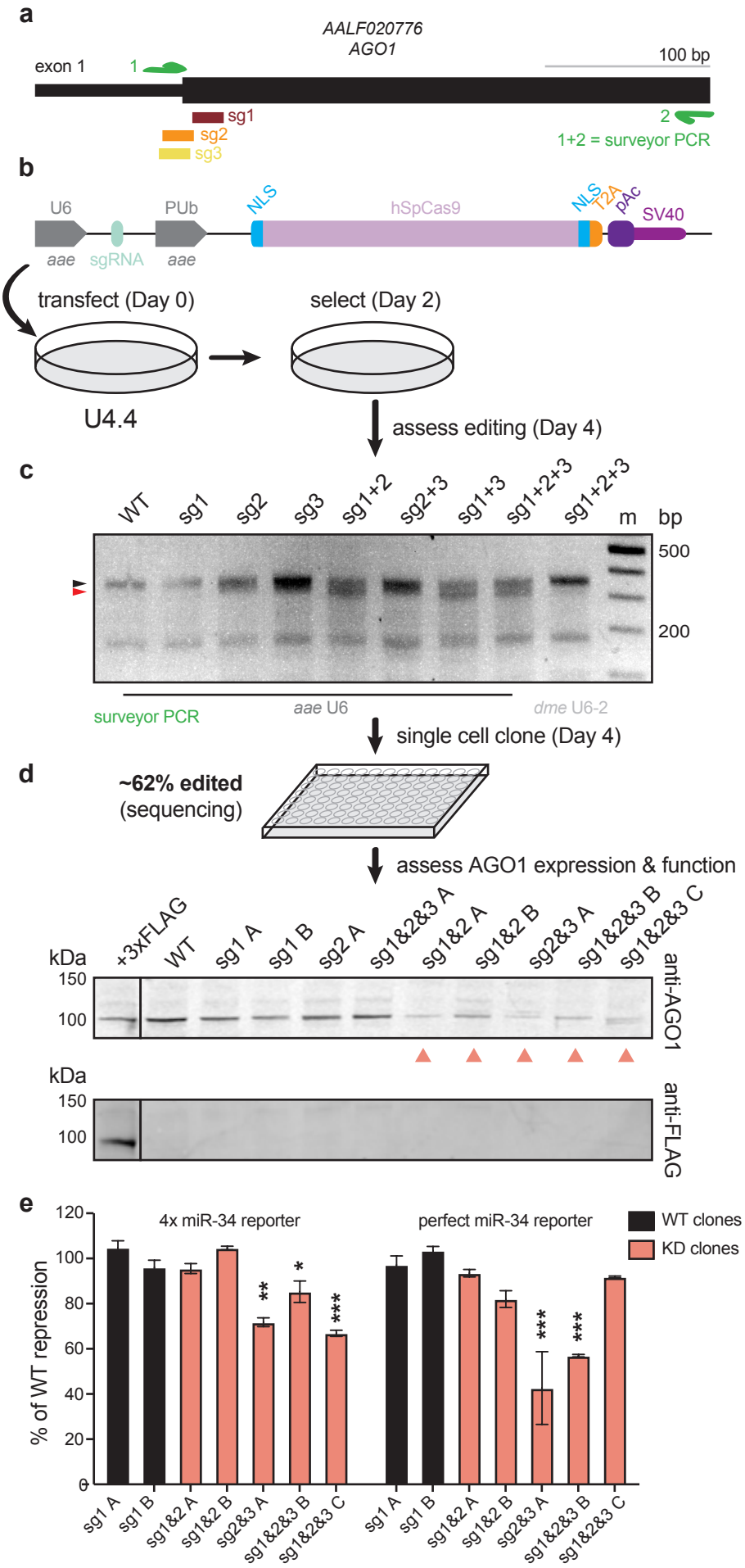

Figure 3. Isolation of AGO1 knock-down U4.4 clonal cell lines.

(a) Three sgRNAs were designed near the translation start site for the *AGO1* locus in U4.4 cells. Note that this diagram shown differs from the *Ae. albopictus* annotation (AaloF1.2) and is based on sequencing of U4.4 cells. A PCR was designed for surveyor assay to asses editing efficiency (primers = green arrows).

(b) U4.4 *AGO1* sgRNAs were cloned into pKRG3, and U4.4 cells were transfected with these plasmids singly or in combination. Day 2 post-transfection, cells were selected with puromycin until Day 4.

(c) Following selection, the surveyor PCR in (a) was used to assess editing by surveyor assay. Expected size of wild-type (WT) amplicon = ~350 base pairs (bp; black arrow); expected size of digested fragments based on sgRNA cleavage site = ~330 (red arrow) + ~23 (not visible), In comparison to the *aae* U6 promoter, no editing is observed with the same guides using the *dme* U6-2 promoter (both plasmids express hSpCas9 using PUb promoter). m = marker. Full-length gels in Supplementary Fig. 3.

(d) Single cells clones were sequenced to assess the percentage of edited clones. Immunoblot of AGO1 (top) showed clones with WT and reduced (salmon arrows) AGO1 protein levels. The ectopically expressed, 3xFLAG-tagged U4.4 AGO1was detected by the endogenous AGO1 antibody and anti-FLAG antibody (bottom). Full-length blots in Supplementary Fig. 3.

(e) Luciferase reporter assay measuring miR-34 mediated repression of 4 repeated ideal miR-34 sites (4x miR-34 reporter) or a perfect miR-34 site (perfect miR-34 reporter). Repression for each clone was measured by normalizing to internal transfection controls (reporter luciferase/control luciferase), then to empty, completely unrepressed reporters in the same clone. The percent (%) of repression compared to WT clones sg1 A and sg1 B is shown. $P < 0.0001$ (overall ANOVA comparing different transfections); individual groups were compared using the Dunnett's *post hoc* test compared to the WT clone sg1 A; *$p < 0.05$, **$P < 0.001$, ***$P \leq 0.0001$.

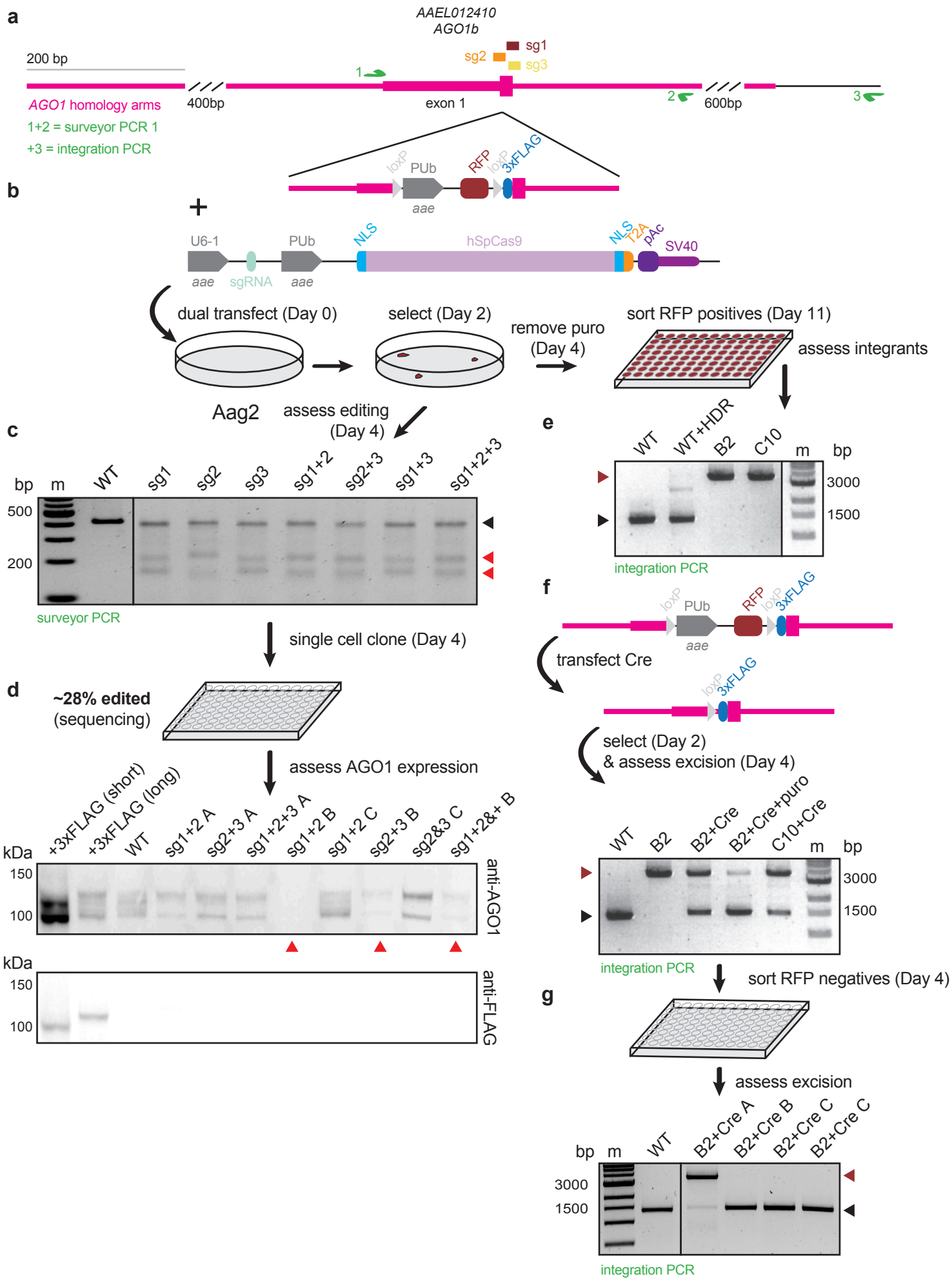
a
AAEL012410
AGO1b
200 bp
sg1
sg2
sg3
1
2
3
AGO1 homology arms
400bp
exon 1
600bp
1+2 = surveyor PCR 1
+3 = integration PCR
loxP
PUb
RFP
loxP
3xFLAG
aae
b
+
U6-1
PUb
NLS
hSpCas9
NLS
T2A
pAc
SV40
aae
sgRNA
aae
dual transfect (Day 0)
select (Day 2)
remove puro
(Day 4)
sort RFP positives (Day 11)
assess integrants
Aag2
assess editing
(Day 4)
c
bp
m
WT
sg1
sg2
sg3
sg1+2
sg2+3
sg1+3
sg1+2+3
500
200
surveyor PCR
single cell clone (Day 4)
d
~28% edited
(sequencing)
assess AGO1 expression
+3xFLAG (short)
+3xFLAG (long)
WT
sg1+2 A
sg2+3 A
sg1+2+3 A
sg1+2 B
sg1+2 C
sg2+3 B
sg2&3 C
sg1+2&+ B
kDa
150
100
anti-AGO1
kDa
150
100
anti-FLAG
e
WT
WT+HDR
B2
C10
m
bp
3000
1500
integration PCR
f
loxP
PUb
RFP
loxP
3xFLAG
aae
transfect Cre
loxP
3xFLAG
select (Day 2)
& assess excision (Day 4)
WT
B2
B2+Cre
B2+Cre+puro
C10+Cre
m
bp
3000
1500
integration PCR
g
sort RFP negatives (Day 4)
assess excision
bp
m
WT
B2+Cre A
B2+Cre B
B2+Cre C
B2+Cre C
3000
1500
integration PCR

527 **References**

528 1 Kraemer, M. U. G. *et al.* Past and future spread of the arbovirus vectors Aedes aegypti and
529 Aedes albopictus. *Nature microbiology* **4**, 854-863, doi:10.1038/s41564-019-0376-y (2019).
530 2 Huang, Y.-J. S., Higgs, S. & Vanlandingham, D. L. Emergence and re-emergence of
531 mosquito-borne arboviruses. *Current Opinion in Virology* **34**, 104-109,
532 doi:https://doi.org/10.1016/j.coviro.2019.01.001 (2019).
533 3 World Health Organization. *WHO Fact Sheet: Vector-Borne Diseases*,
534 <https://www.who.int/news-room/fact-sheets/detail/vector-borne-diseases> (2020).
535 4 Schuffenecker, I. *et al.* Genome microevolution of chikungunya viruses causing the Indian
536 Ocean outbreak. *PLoS medicine* **3**, e263, doi:10.1371/journal.pmed.0030263 (2006).
537 5 Tsetsarkin, K. A., Vanlandingham, D. L., McGee, C. E. & Higgs, S. A single mutation in
538 chikungunya virus affects vector specificity and epidemic potential. *PLoS pathogens* **3**, e201,
539 doi:10.1371/journal.ppat.0030201 (2007).
540 6 Windbichler, N. *et al.* A synthetic homing endonuclease-based gene drive system in the
541 human malaria mosquito. *Nature* **473**, 212-215, doi:10.1038/nature09937 (2011).
542 7 Hammond, A. M. *et al.* The creation and selection of mutations resistant to a gene drive over
543 multiple generations in the malaria mosquito. *PLoS Genet* **13**, e1007039,
544 doi:10.1371/journal.pgen.1007039 (2017).
545 8 Buchman, A. *et al.* Broad dengue neutralization in mosquitoes expressing an engineered
546 antibody. *PLOS Pathogens* **16**, e1008103, doi:10.1371/journal.ppat.1008103 (2020).
547 9 Lobo, N. F., Hua-Van, A., Li, X., Nolen, B. M. & Fraser, M. J., Jr. Germ line transformation of
548 the yellow fever mosquito, Aedes aegypti, mediated by transpositional insertion of a piggyBac
549 vector. *Insect Mol Biol* **11**, 133-139, doi:10.1046/j.1365-2583.2002.00317.x (2002).
550 10 Coates, C. J., Jasinskiene, N., Miyashiro, L. & James, A. A. Mariner transposition and
551 transformation of the yellow fever mosquito, Aedes aegypti. *Proc Natl Acad Sci U S A* **95**,
552 3748-3751, doi:10.1073/pnas.95.7.3748 (1998).
553 11 Ivics, Z. *et al.* Transposon-mediated genome manipulation in vertebrates. *Nat Methods* **6**, 415-
554 422, doi:10.1038/nmeth.1332 (2009).
555 12 Aryan, A., Myles, K. M. & Adelman, Z. N. Targeted genome editing in Aedes aegypti using
556 TALENs. *Methods* **69**, 38-45, doi:https://doi.org/10.1016/j.ymeth.2014.02.008 (2014).
557 13 Aryan, A., Anderson, M. A. E., Myles, K. M. & Adelman, Z. N. TALEN-Based Gene Disruption
558 in the Dengue Vector Aedes aegypti. *PLOS ONE* **8**, e60082,
559 doi:10.1371/journal.pone.0060082 (2013).
560 14 DeGennaro, M. *et al.* orco mutant mosquitoes lose strong preference for humans and are not
561 repelled by volatile DEET. *Nature* **498**, 487-491, doi:10.1038/nature12206 (2013).
562 15 McMeniman, Conor J., Corfas, Román A., Matthews, Benjamin J., Ritchie, Scott A. &
563 Vosshall, Leslie B. Multimodal Integration of Carbon Dioxide and Other Sensory Cues Drives
564 Mosquito Attraction to Humans. *Cell* **156**, 1060-1071, doi:10.1016/j.cell.2013.12.044 (2014).
565 16 Liesch, J., Bellani, L. L. & Vosshall, L. B. Functional and genetic characterization of
566 neuropeptide Y-like receptors in Aedes aegypti. *PLoS neglected tropical diseases* **7**, e2486-
567 e2486, doi:10.1371/journal.pntd.0002486 (2013).
568 17 Carroll, D. Genome engineering with targetable nucleases. *Annu Rev Biochem* **83**, 409-439,
569 doi:10.1146/annurev-biochem-060713-035418 (2014).
570 18 Aryan, A., Anderson, M. A. E., Myles, K. M. & Adelman, Z. N. Germline excision of transgenes
571 in Aedes aegypti by homing endonucleases. *Sci Rep* **3**, 1603-1603, doi:10.1038/srep01603
572 (2013).
573 19 Stoddard, B. L. Homing endonucleases from mobile group I introns: discovery to genome
574 engineering. *Mob DNA* **5**, 7-7, doi:10.1186/1759-8753-5-7 (2014).
575 20 Nene, V. *et al.* Genome sequence of Aedes aegypti, a major arbovirus vector. *Science* **316**,
576 1718-1723, doi:10.1126/science.1138878 (2007).

21 Timoshevskiy, V. A. *et al.* Genomic composition and evolution of Aedes aegypti chromosomes revealed by the analysis of physically mapped supercontigs. *BMC Biol* **12**, 27, doi:10.1186/1741-7007-12-27 (2014).
22 Juneja, P. *et al.* Assembly of the genome of the disease vector Aedes aegypti onto a genetic linkage map allows mapping of genes affecting disease transmission. *PLoS Negl Trop Dis* **8**, e2652, doi:10.1371/journal.pntd.0002652 (2014).
23 Matthews, B. J. *et al.* Improved reference genome of Aedes aegypti informs arbovirus vector control. *Nature* **563**, 501-507, doi:10.1038/s41586-018-0692-z (2018).
24 Doudna, J. A. & Charpentier, E. Genome editing. The new frontier of genome engineering with CRISPR-Cas9. *Science* **346**, 1258096, doi:10.1126/science.1258096 (2014).
25 Jinek, M. *et al.* A Programmable Dual-RNA–Guided DNA Endonuclease in Adaptive Bacterial Immunity. *Science* **337**, 816-821, doi:10.1126/science.1225829 (2012).
26 Mali, P. *et al.* RNA-Guided Human Genome Engineering via Cas9. *Science* **339**, 823-826, doi:10.1126/science.1232033 (2013).
27 Jinek, M. *et al.* RNA-programmed genome editing in human cells. *Elife* **2**, e00471, doi:10.7554/eLife.00471 (2013).
28 Peng, Y. *et al.* Making designer mutants in model organisms. *Development* **141**, 4042-4054, doi:10.1242/dev.102186 (2014).
29 Gokcezade, J., Sienski, G. & Duchek, P. Efficient CRISPR/Cas9 Plasmids for Rapid and Versatile Genome Editing in *Drosophila*. *G3: Genes|Genomes|Genetics* **4**, 2279-2282, doi:10.1534/g3.114.014126 (2014).
30 Bassett, A. R., Tibbit, C., Ponting, C. P. & Liu, J.-L. Mutagenesis and homologous recombination in *Drosophila* cell lines using CRISPR/Cas9. *Biology Open* **3**, 42-49, doi:10.1242/bio.20137120 (2014).
31 Hwang, W. Y. *et al.* Efficient genome editing in zebrafish using a CRISPR-Cas system. *Nat Biotechnol* **31**, 227-229, doi:10.1038/nbt.2501 (2013).
32 Kistler, K. E., Vosshall, L. B. & Matthews, B. J. Genome engineering with CRISPR-Cas9 in the mosquito *Aedes aegypti*. *Cell Rep* **11**, 51-60, doi:10.1016/j.celrep.2015.03.009 (2015).
33 Liu, P. *et al. Nix* is a male-determining factor in the Asian tiger mosquito *Aedes albopictus*. *Insect Biochemistry and Molecular Biology* **118**, 103311, doi:https://doi.org/10.1016/j.ibmb.2019.103311 (2020).
34 Suzuki, Y. *et al.* Non-retroviral Endogenous Viral Element Limits Cognate Virus Replication in *Aedes aegypti* Ovaries. *Current Biology* **30**, 3495-3506.e3496, doi:10.1016/j.cub.2020.06.057 (2020).
35 Dong, S. *et al.* Heritable CRISPR/Cas9-Mediated Genome Editing in the Yellow Fever Mosquito, Aedes aegypti. *PLOS ONE* **10**, e0122353, doi:10.1371/journal.pone.0122353 (2015).
36 Li, M. *et al.* Development of a confinable gene drive system in the human disease vector Aedes aegypti. *eLife* **9**, e51701, doi:10.7554/eLife.51701 (2020).
37 Hillary, V. E., Ceasar, S. A. & Ignacimuthu, S. in *Genome Engineering via CRISPR-Cas9 System* (eds Vijai Singh & Pawan K. Dhar) 219-249 (Academic Press, 2020).
38 Fredericks, A. C. *et al. Aedes aegypti* (Aag2)-derived clonal mosquito cell lines reveal the effects of pre-existing persistent infection with the insect-specific bunyavirus Phasi Charoen-like virus on arbovirus replication. *PLOS Neglected Tropical Diseases* **13**, e0007346, doi:10.1371/journal.pntd.0007346 (2019).
39 Varjak, M. *et al. Aedes aegypti* Piwi4 Is a Noncanonical PIWI Protein Involved in Antiviral Responses. *mSphere* **2**, doi:10.1128/mSphere.00144-17 (2017).
40 Lan, Q. & Fallon, A. M. Small heat shock proteins distinguish between two mosquito species and confirm identity of their cell lines. *The American journal of tropical medicine and hygiene* **43**, 669-676 (1990).

627 41 Barletta, A. B. F., Silva, M. C. L. N. & Sorgine, M. H. F. Validation of Aedes aegypti Aag-2
628 cells as a model for insect immune studies. *Parasites & Vectors* **5**, 148, doi:10.1186/1756-
629 3305-5-148 (2012).
630 42 Siu, R. W. *et al.* Antiviral RNA interference responses induced by Semliki Forest virus infection
631 of mosquito cells: characterization, origin, and frequency-dependent functions of virus-derived
632 small interfering RNAs. *J Virol* **85**, 2907-2917, doi:10.1128/JVI.02052-10 (2011).
633 43 Condreay, L. D. & Brown, D. T. Exclusion of superinfecting homologous virus by Sindbis virus-
634 infected Aedes albopictus (mosquito) cells. *Journal of Virology* **58**, 81-86 (1986).
635 44 Gratz, S. J. *et al.* Genome engineering of *Drosophila* with the CRISPR RNA-guided Cas9
636 nuclease. *Genetics* **194**, 1029-1035, doi:10.1534/genetics.113.152710 (2013).
637 45 Wakiyama, M., Matsumoto, T. & Yokoyama, S. *Drosophila* U6 promoter-driven short hairpin
638 RNAs effectively induce RNA interference in Schneider 2 cells. *Biochem Biophys Res*
639 *Commun* **331**, 1163-1170, doi:10.1016/j.bbrc.2005.03.240 (2005).
640 46 Xue, Z. *et al.* Efficient gene knock-out and knock-in with transgenic Cas9 in Drosophila. *G3*
641 *(Bethesda)* **4**, 925-929, doi:10.1534/g3.114.010496 (2014).
642 47 Ren, X. *et al.* Optimized gene editing technology for *Drosophila melanogaster* using germ line-
643 specific Cas9. *Proceedings of the National Academy of Sciences* **110**, 19012-19017,
644 doi:10.1073/pnas.1318481110 (2013).
645 48 Kondo, S. & Ueda, R. Highly Improved Gene Targeting by Germline-Specific Cas9 Expression
646 in *Drosophila*. *Genetics* **195**, 715-721, doi:10.1534/genetics.113.156737 (2013).
647 49 Loukeris, T. G. *Use of the Minos transposable element from Drosophila hydei as a gene*
648 *transfer vector for Diptera.*, University of Crete, Greece, (1996).
649 50 Cong, L. *et al.* Multiplex Genome Engineering Using CRISPR/Cas Systems. *Science* **339**,
650 819, doi:10.1126/science.1231143 (2013).
651 51 Anderson, M. A. E., Gross, T. L., Myles, K. M. & Adelman, Z. N. Validation of novel promoter
652 sequences derived from two endogenous ubiquitin genes in transgenic Aedes aegypti. *Insect*
653 *molecular biology* **19**, 441-449, doi:10.1111/j.1365-2583.2010.01005.x (2010).
654 52 Lycett, G. J. & Crampton, J. M. Stable transformation of mosquito cell lines using a *hsp70::neo*
655 fusion gene. *Gene* **136**, 129-136, doi:https://doi.org/10.1016/0378-1119(93)90456-D (1993).
656 53 Anderson, M. A. E. *et al.* Expanding the CRISPR Toolbox in Culicine Mosquitoes: *In Vitro*
657 Validation of Pol III Promoters. *ACS Synthetic Biology* **9**, 678-681,
658 doi:10.1021/acssynbio.9b00436 (2020).
659 54 Konet, D. S. *et al.* Short-hairpin RNA expressed from polymerase III promoters mediates RNA
660 interference in mosquito cells. *Insect Mol Biol* **16**, 199-206, doi:10.1111/j.1365-
661 2583.2006.00714.x (2007).
662 55 Donnelly, M. L. L. *et al.* The 'cleavage' activities of foot-and-mouth disease virus 2A site-
663 directed mutants and naturally occurring '2A-like' sequences. *Journal of General Virology* **82**,
664 1027-1041, doi:https://doi.org/10.1099/0022-1317-82-5-1027 (2001).
665 56 González, M. *et al.* Generation of stable *Drosophila* cell lines using multicistronic vectors. *Sci*
666 *Rep* **1**, 75-75, doi:10.1038/srep00075 (2011).
667 57 Varjak, M. *et al.* Characterization of the Zika virus induced small RNA response in *Aedes*
668 *aegypti* cells. *PLOS Neglected Tropical Diseases* **11**, e0006010,
669 doi:10.1371/journal.pntd.0006010 (2017).
670 58 Diao, F. & White, B. H. A Novel Approach for Directing Transgene Expression in *Drosophila*:
671 T2A-Gal4 In-Frame Fusion. *Genetics* **190**, 1139-1144, doi:10.1534/genetics.111.136291
672 (2012).
673 59 Bartel, D. P. Metazoan MicroRNAs. *Cell* **173**, 20-51, doi:10.1016/j.cell.2018.03.006 (2018).
674 60 Luna, Joseph M. *et al.* Hepatitis C Virus RNA Functionally Sequesters miR-122. *Cell* **160**,
675 1099-1110, doi:https://doi.org/10.1016/j.cell.2015.02.025 (2015).

676 **Acknowledgements**

677

678 We thank the Rockefeller University Flow Cytometry Resource Center; and M.E. Castillo, S.M.
679 Pecoraro Di Vittorio, A. Norris, S. Shirley, A. O'Connell, and G. Santiago for excellent technical
680 and administrative assistance. We thank the members of the Rice and Vosshall labs and C.
681 McMeniman for invaluable advice, reagents, and discussions. This study was supported by
682 NIH/NIAID grants R01-AI116943 (C.M.R., S.Y, E.J, K.R.G). K.R.G was supported by the
683 Rockefeller University Women and Science Fellowship and a Ruth L. Kirschstein National
684 Research Service Award (NIAID/NIH F32-AI120579).

685

686 **Author Contributions**

687

688 K.R.G and C.M.R. designed the project and experiments. K.R.G., S.Y., E.J., and S.N. performed
689 experiments. K.R.G. performed data analysis and wrote the manuscript with input from all authors.

690

691 **Additional Information**

692

693 The authors declare no competing interests.

694

695 **Figure legends**

696

697 **Figure 1. Mosquito optimized CRISPR/Cas9 plasmids.**

698

699 (a) pDCC6 plasmid published in Gokcezade et al., 2014. The *dme* U6-2 promoter drives sgRNA
700 transcription and the *dme* phsp70 promoter drives expression of a 3xFLAG-tagged hSpCas9.
701 Guide RNAs are cloned by *BbsI* digest.

702

703 (b) pKRG2 plasmid, generated by replacing the *dme* phsp70 promoter with the *aae* PUb promoter.
704 Cloning of guide RNAs as in (a).

705

706 (c) Immunoblot of Aag2 cells treated with transfection reagent (ctrl) or transfected with pDCC6
707 (3xFLAG-hSpCas9; expressed from the *dme* pshp70 promoter) or with pKRG2 (3xFLAG-
708 hSpCas9; expressed from the PUb promoter). kDa = kilodaltons. Full-length blots in
709 Supplementary Fig. 3.

710

711 (d) As in (c) for U4.4 cells.

712

713 (e) To generate pKRG3 mosquito adapted plasmids, the pKRG2 guide RNA cloning site was
714 redesigned to use *BsmBI* (allowing insertion of the *aae* U6 promoter, which is incompatible with
715 the *BbsI* sgRNA cloning site). The RNA Pol II *aae* U6 promoter was then inserted to express
716 sgRNAs. This plasmid was further modified by removing the N-terminal 3xFLAG from Cas9 and
717 adding a T2A-pAc to allow puromycin selection to yield several options for mosquito optimized
718 CRISPR/Cas9 editing.

719

720 **Figure 2. Efficient puromycin selection of hSpCas9-pAc transfected mosquito cells.**

721

722 (a) Aag2 cells were pre-treated with transfection reagent alone (puro), transfected with a control
723 PUb-eCFP (enhanced cyan fluorescent protein) plasmid lacking a puromycin resistance cassette
724 (puro + eCFP), or transfected with PUb-hSpCas9 linked to a puromycin resistance cassette by
725 thes T2A skipping site (hSpCas9-pAc). Day 2 post-transfection, cells were treated with 2.5 ug/mL
726 puro (puromycin). $P < 0.0001$ (overall ANOVA comparing different transfections); individual

727 groups were compared using the Dunnett's *post hoc* test compared to the puro control; **P <
728 0.001, ***P ≤ 0.0001.
729
730 (b) As in (a) for U4.4 cells treated with 10 ug/mL puro. *P < 0.05, ***P ≤ 0.0001.
731
732 (c) Immunoblot of Aag2 cells treated with transfection reagent alone (ctrl) or transfected with
733 hSpCas9 or hSpCas9-pAc (driven by PUb promoter). Expected size of hSpCas9 is ~160
734 kilodaltons (kDa); expected size of unprocessed hSpCas9-pAc is ~185 kDa. Full-length blots in
735 Supplementary Fig. 3.
736
737 (d) As in (c) for U4.4 cells.
738
739 **Figure 3. Isolation of AGO1 knock-down U4.4 clonal cell lines.**
740
741 (a) Three sgRNAs were designed near the translation start site for the *AGO1* locus in U4.4 cells.
742 Note that this diagram shown differs from the *Ae. albopictus* annotation (AaloF1.2) and is based
743 on sequencing of U4.4 cells. A PCR was designed for surveyor assay to assess editing efficiency
744 (primers = green arrows).
745
746 (b) U4.4 *AGO1* sgRNAs were cloned into pKRG3, and U4.4 cells were transfected with these
747 plasmids singly or in combination. Day 2 post-transfection, cells were selected with puromycin
748 until Day 4.
749
750 (c) Following selection, the surveyor PCR in (a) was used to assess editing by surveyor assay.
751 Expected size of wild-type (WT) amplicon = ~350 base pairs (bp; black arrow); expected size of

752 digested fragments based on sgRNA cleavage sites = ~330 (red arrow) + ~23 (not visible), In
753 comparison to the *aae* U6 promoter, no editing is observed with the same guides using the *dme*
754 U6-2 promoter (both plasmids express hSpCas9 using PUb promoter). m = marker. Full-length
755 gels in Supplementary Fig. 3.
756
757 (d) Single cells clones were sequenced to assess the percentage of edited clones. Immunoblot
758 of AGO1 (top) showed clones with WT and reduced (salmon arrows) AGO1 protein levels. The
759 ectopically expressed, 3xFLAG-tagged U4.4 AGO1 was detected by the endogenous AGO1
760 antibody and anti-FLAG antibody (bottom). Full-length blots in Supplementary Fig. 3.
761
762 (e) Luciferase reporter assay measuring miR-34 mediated repression of 4 repeated ideal miR-34
763 sites (4x miR-34 reporter) or a perfect miR-34 site (perfect miR-34 reporter). Repression for each
764 clone was measured by normalizing to internal transfection controls (reporter luciferase/control
765 luciferase), then to empty, completely unrepressed reporters in the same clone. The percent (%)
766 of repression compared to WT clones sg1 A and sg1 B is shown. $P < 0.0001$ (overall ANOVA
767 comparing different transfections); individual groups were compared using the Dunnett's *post hoc*
768 test compared to the WT clone sg1 A; *$p < 0.05$, **$P < 0.001$, ***$P \leq 0.0001$.
769
770 **Figure 4. CRISPR/Cas9 mediated editing and knock-in of *AGO1* in Aag2 cells.**
771
772 (a) Three sgRNAs (sg) were designed near the *AGO1* translation start site in Aag2 cells. A PCR
773 was designed for surveyor assay to assess editing efficiency (green arrows 1 and 2). *AGO1*
774 homology arms are indicated; an additional reverse primer was designed outside the homology
775 region (green arrow 3).
776

777 (b) Homology-directed repair (HDR) donor template design. Upstream of the coding sequence,
778 the PUb promoter expresses red fluorescent protein (RFP); PUb-RFP is flanked by two loxP sites.
779 Aag2 *AGO1* sgRNAs were cloned into pKRG3, and cells were transfected with these plasmids
780 and the HDR donor template. Day 2 post-transfection, cells were selected with puromycin (puro)
781 until Day 4 then screened for editing efficiency. Alternatively, puro selection was removed (Day
782 4) and cells were cultured until Day 11 and sorted for RFP-positive clones.
783
784 (c) Following selection, the surveyor PCR in (a) was used to assess editing efficiency by surveyor
785 assay. Expected size of wild-type (WT) amplicon = ~410 base pairs (bp; black arrow); expected
786 size of digested fragments based on sgRNA cleavage sites = ~180 + ~230 (red arrow); m =
787 marker. Full-length gels in Supplementary Fig. 3.
788
789 (d) Single cell clones were sequenced to determine the percentage of edited clones. Immunoblot
790 of AGO1 (top) showed clones with WT and reduced (red arrows) AGO1 protein levels. The
791 ectopically expressed, 3xFLAG-tagged Aag2 AGO1 short isoform and the 3xFLAG-tagged Aag2
792 AGO1 long isoform expressed from a stable Aag2 cell line were detected by the endogenous
793 AGO1 antibody and anti-FLAG antibody (bottom). Full-length blots in Supplementary Fig. 3.
794
795 (e) RFP positive Aag2 cell clones from (b) were screened for HDR mediated integration of the
796 donor template by the integration PCR in (a). Expected size of amplicons from WT clones = ~1500
797 base pairs (bp; black arrow); expected size of amplicons from clones containing the integrated
798 HDR donor template = ~3,700 bp (dark red arrow). Control WT cells freshly transfected with the
799 HDR donor template (WT+HDR) ensure the donor template is not detected by the integration
800 PCR. B2 and C10 clones were knock-in at the *AGO1* locus. Full-length gels in Supplementary
801 Fig. 3.
802

803 (f) The PUb-RFP cassette was excised from Aag2 *AGO1* knock-in clones (B2 and C10) by
804 transfection of PUb-driven Cre-T2A-pAc. Transfected cells were selected with puro and the
805 integration PCR in (a) was used to assess excision. WT and transfected B2 cells are shown;
806 expected amplicon sizes as in (e); expected size of Cre excised amplicon = ~1500 base pairs
807 (bp; black arrow). Puro treatment increases the proportion of Cre exicision (B2+Cre+puro). Full-
808 length gels in Supplementary Fig. 3.
809
810 (g) B2 and C10 Cre excised cell lines were sorted for RFP negative cells and subcloned lines
811 were again screened for homozygous knock-in 3xFLAG-*AGO1* Aag2 cell lines with the integration
812 PCR in (a). Expected amplicon sizes as in (e-f); base pairs = bp. Full-length gels in Supplementary
813 Fig. 3.
814
815 **Supplementary Figure Titles and Legends**
816
817 **Supplementary Figure 1. Efficient transfection of mosquito cells.** (provided in Supplementary
818 Information file)
819
820 (a) Representative merged brightfield and CFP image for control (ctrl) U4.4 cells treated with
821 transfection reagent alone.
822
823 (b) As in (b), for cells transfected with PUb-eCFP.
824
825 **Supplementary Figure 2. *AGO1* sequences of single cell clones isolated after CRISPR/Cas9**
826 **transfection.** (provided in Supplementary Information file)
827

828 (a) Representative alignment of *AGO1* sequences from established U4.4 single cell clones.
829 Clones were isolated and sequenced post-transfection with pKRG3 CRISPR/Cas9 plasmids
830 containing guides targeting *AGO1*. sgRNA cleavage sites = red arrows; starting methionine =
831 black box.
832
833 (b) As in (a), for Aag2 cells.
834
835 **Supplementary Figure 3. Full-length blots and gels.** (provided in Supplementary Information
836 file)
837
838 (a-j) Full-length blots and gels for all Figures.
839
840 **Supplementary Table Titles and Legends**
841
842 **Supplementary Table 1. Sequences of all oligos used in this study.** (provided in
843 Supplementary Information file)
844
845 HA = homology arm; HDR = homology-directed repair; tracr = trans-activating CRISPR; sgRNA
846 = single-guide RNA. All oligos were ordered in standard desalted format from IDT, unless
847 indicated otherwise.